ENVIRONMENTAL BIOTECHNOLOGY

Cadmium removal and 2,4-dichlorophenol degradation by immobilized *Phanerochaete chrysosporium* loaded with nitrogen-doped TiO$_2$ nanoparticles

**Guiqiu Chen · Song Guan · Guangming Zeng ·
Xiaodong Li · Anwei Chen · Cui Shang · Ying Zhou ·
Huanke Li · Jianmin He**

Abstract *Phanerochaete chrysosporium* has been identified as an effective bioremediation agent for its biosorption and degradation ability. However, the applications of *P. chrysosporium* are limited owing to its long degradation time and low resistance to pollutants. In this research, nitrogen-doped TiO$_2$ nanoparticles were loaded on *P. chrysosporium* to improve the remediation capacity for pollutants. The removal efficiencies were maintained at a high level: 84.2 % for Cd(II) and 78.9 % for 2,4-dichlorophenol (2,4-DCP) in the wide pH range of 4.0 to 7.0 in 60 h. The removal capacity of immobilized *P. chrysosporium* loaded with nitrogen-doped TiO$_2$ nanoparticles (PTNs) was strongly affected by the initial Cd(II) and 2,4-DCP concentrations. The hyphae of PTNs became tight, and a large amount of crystals adhered to them after the reaction. Fourier transform infrared spectroscopy showed that carboxyl, amino, and hydroxyl groups on the surface of PTNs were responsible for the biosorption. In the degradation process, 2,4-DCP was broken down into *o*-chlorotoluene and 4-hexene-1-ol. These results showed that PTNs is promising for simultaneous removal of Cd(II) and 2,4-DCP from wastewater.

G. Chen (✉) · S. Guan · G. Zeng (✉) · X. Li · A. Chen ·
C. Shang · Y. Zhou · H. Li · J. He
College of Environmental Science and Engineering,
Hunan University,
Changsha 410082, People's Republic of China
e-mail: gqchen@hnu.edu.cn
e-mail: zgming@hnu.edu.cn

G. Chen · S. Guan · G. Zeng · X. Li · A. Chen · C. Shang ·
Y. Zhou · H. Li · J. He
Key Laboratory of Environmental Biology and Pollution Control
(Hunan University), Ministry of Education,
Changsha 410082, People's Republic of China

Introduction

An increasing amount of toxic inorganic and organic wastes are being discharged into the environment, causing serious water, air, and soil pollution nowadays (Sayari et al. 2005). The compound pollutions of heavy metals and organics have aroused wide public concern because they are more harmful to human beings and are more difficult to remove (Chen et al. 2011a; Zumriye and Gönen 2006). Cd(II) and its organic co-pollutants are often produced from industrial processes such as leather tanning, photographic-film manufacturing, wood preservation, car manufacturing, and petroleum refining and agricultural activities. Cd(II) is one of the most toxic heavy metals, which mainly comes from processes such as electroplating, smelting, and mining. It accumulates easily in living organisms and is harmful to the kidneys, liver, and the skeletal system (Chen et al. 2008; Xiao et al. 2010). 2,4-Dichlorophenol (2,4-DCP), a widely distributed chlorophenol contaminant, has also been used as a wood preservative, pesticide, and fungicide besides being used in anticorrosive rust production. 2,4-DCP causes strong caustic and denaturing effects on organisms, including irritation of the skin and the mucous membrane (Andreozzi et al. 2011; Yin et al. 2010b). The composite pollutants containing Cd(II) and 2,4-DCP can be more toxic and more difficult to remove than the single one. Although many studies have investigated the disposal of heavy metals or chlorophenols, respectively, little research has focused on the simultaneous removal of these two kinds of pollutants.

Bioremediation using microorganisms offers an attractive option in treating wastewater containing composite pollutants of Cd(II) and 2,4-DCP instead of the traditional processes. *P. chrysosporium* has been reported as an effective biomass used for degrading xenobiotics and adsorbing heavy metals (Bakircioglu et al. 2010; Chen et al. 2011a, b; Huang et al. 2008). However, the application of *P. chrysosporium* is limited owing to its long degradation time and low resistance to pollutants (Zouari et al. 2002). If some materials be added to enhance the resistance of *P. chrysosporium* to the toxic pollutants, to shorten its degradation time, and to improve the disposal efficiency, it could be a promising material to the wastewater treatment.

One environmentally friendly technology for water treatment, semiconductor photocatalysis, has recently attracted substantial attention for its advantages over conventional processes (Brezová et al. 2009). TiO$_2$ nanoparticle is one of the most popular photocatalysts because of its high physical and chemical stability, non-toxicity, and low cost (Wodka et al. 2010). When TiO$_2$ nanoparticles are illuminated by light with wavelengths shorter than 380 nm, photons can excite valence band electrons across the band gap into the conduction band, leaving holes in the valence band. These holes react with water molecules or hydroxide ions and produce hydroxyl radicals, which play a major role in the process of organics degradation in wastewater (Doong et al. 2001; Gimeno et al. 2007; Zhang et al. 2009).

However, most wavelengths of solar energy that arrive on earth are longer than 380 nm, which greatly reduces the degradation ability of TiO$_2$ nanoparticles (Asahi et al. 2001). At present, reductive hydrogen plasma treatment, dye sensitization, transition metal doping, and non-metal doping are the main methods used to induce TiO$_2$ nanoparticles to yield high reactivity under visible light (Jo and Kim 2009). Among them, non-metal N-doping was chosen in this study to enhance the performance of TiO$_2$ nanoparticles and to overcome the limitations of other methods, such as photocorrosion and limited long-term stability (Wodka et al. 2010; Yin et al. 2010a).

Owing to the mentioned reasons above, nitrogen-doped TiO$_2$ nanoparticles were loaded onto *P. chrysosporium* immobilizing with sodium alginate gel to dispose of wastewater containing Cd(II) and 2,4-DCP. The effects of contact time, pH, and initial concentrations were examined in batch experiments. Scanning electron microscopy (SEM), energy-dispersive X-ray analysis (EDAX), Fourier transform infrared spectrometry (FT-IR), and gas chromatography–mass spectrometry (GC–MS) were conducted to understand the removal pathways and mechanisms of immobilized *P. chrysosporium* loaded with nitrogen-doped TiO$_2$ nanoparticles (PTNs). The current study demonstrated that PTNs could increase the resistance of *P. chrysosporium* to the toxic effects of pollutants and shorten its degradation time.

The experimental results provided essential informations on the application of PTNs in the treatment of Cd(II) and 2,4-DCP composite wastewater.

Materials and methods

Microorganism and reagents

The *P. chrysosporium* BKM-F1767 (ATCC 24725) used in this study was purchased from the China Center for Type Culture Collection (Wuhan, China). Kirk's liquid culture medium was used in a 250-mL Erlenmeyer flask. The strain was inoculated on the culture medium for 7 days at 37 °C. Mycelial suspensions were obtained by dissolving the spores into sterile distilled water, and the spore concentration was adjusted to 1.0×10^5 CFU/mL using a turbidimeter (WGZ-200, Shanghai, China).

2,4-DCP (analytically pure) was purchased from Tianjin Guangfu Fine Chemical Research Institute (Tianjin, China). All other inorganic and organic chemicals were of analytical grade and were purchased from Shanghai First Reagent Co., China. One thousand milligrams per liter of Cd(II) was prepared as the experimental stock solution by dissolving Cd (NO$_3$)$_2$·4H$_2$O in ultrapure water. A 2,4-DCP stock solution was prepared by dissolving 0.5 g 2,4-DCP in 1.0 L ultrapure water. The 2,4-DCP stock solution was stored in a brown glass bottle to avoid photodegradation. Test solutions were prepared by diluting the stock solutions to the desired concentrations.

Preparation of nitrogen-doped TiO$_2$ nanoparticles

TiO$_2$ nanoparticles doped with nitrogen were synthesized via sol–gel method using carbamide, tetrabutyl titanate (TT), absolute ethyl alcohol (AEA), glacial acetic acid (GAA), and double distilled water (DDT) as starting materials. A fixed amount of AEA, DDT, and GAA (V$_{TT}$/V$_{DDT}$/V$_{GAA}$=10:2:3) were mixed as solution A. A number of carbamide was then added into solution A (n_{Ti}/n_N=1:10). TT and AEA (V$_{TT}$/V$_{AEA}$=1:4) were mixed to comprise solution B. Solution A was displaced in drops into solution B while applying magnetic stirring. After the titration process, the solution mixture was peptized overnight in the air. The gels were then dried at 80 °C in an oven (DHG-9076A, Shanghai, China) for several hours until yellow block crystals appeared. These crystals were crushed and ground into fine powder using a mortar and pestle, and further calcined at 500 °C in a muffle furnace (SX2-5-12, Shanghai, China) for 2 h (Prasad et al. 2010).

Preparation of immobilized *P. chrysosporium*

P. chrysosporium was immobilized by mixing 20 mL *P. chrysosporium* spore suspension, 20 mL sodium alginate

solution (6.0 %), and 1 g nitrogen-doped TiO$_2$ nanoparticles. The mixture was injected dropwise into a CaCl$_2$ solution (3 %) using an injector to form beads. The beads were hardened in the CaCl$_2$ solution for 2 h to enhance their mechanical stability. Then, the beads were rinsed with ultrapure water and transferred into the culture medium in conical flasks. After 3 days of shaking on a rotary shaker (150 rpm) at 37 °C, the PTNs were collected and rinsed with ultrapure water for use.

Contact time

Contact time was initially examined to determine the equilibrium time required for the following experiments. The initial concentrations of 20 mg/L Cd(II), 10 mg/L 2,4-DCP, and a dose of 9 g/L of PTNs were added to conical flasks containing 100 mL aqueous solution. The pH was adjusted to 6.0 with 0.1 mol/L HCl or 0.1 mol/L NaOH using a pH meter (FE20 Mettler Toledo, Switzerland). The conical flasks were agitated in an incubator (ZHWY, Shanghai, China) at 37 °C with illumination by filament lamp. Subsequently, 5-mL samples were removed from the flasks with the setting time interval and centrifuged in a centrifuger (TGL20-M, Hukang, China) at 10,000 rpm for 10 min. The supernatant was used to analyze the residual Cd(II) and 2,4-DCP concentrations.

Effect of pH

The solutions with 20 mg/L Cd(II), 10 mg/L 2,4-DCP, and a dose of 9 g/L PTNs were used to investigate the effect of pH on Cd(II) biosorption and 2,4-DCP degradation in the pH range of 3.0–8.0, which was adjusted with 0.1 mol/L HNO$_3$ or NaOH at the beginning of the experiment. All flasks were sealed and agitated in the incubator at 37 °C and 150 rpm with illumination by filament lamp. After sufficient contact time (previous experiments showed that 60 h was enough for Cd(II) biosorption and 2,4-DCP degradation), PTNs were separated by filtration.

Effect of initial Cd(II) concentration

A series of Cd(II) solutions with concentrations of 2, 5, 10, 20, 40, 80, 100, and 120 mg/L were prepared to determine the effect of initial Cd(II) concentration on Cd(II) biosorption and 2,4-DCP degradation. The 2,4-DCP concentration in each of the flasks was adjusted to 10 mg/L. The mixtures were adjusted to pH 6.0 with 0.1 mol/L HNO$_3$ or NaOH, and then shaken in the same incubator with illumination by filament lamp. Samples were taken from the flasks at 60 h, and the residual Cd(II) and 2,4-DCP concentrations were analyzed using the aforementioned methods.

Effect of initial 2,4-DCP concentration

To determine the optimal initial 2,4-DCP concentration for the removal process, the initial 2,4-DCP concentration was adjusted to the various values, including 2, 5, 10, 20, 40, 60, 80, and 100 mg/L to evaluate the effect of the initial phenol concentration on the cadmium removal and 2,4-DCP degradation. The initial cadmium concentration in each of the flasks was 2 mg/L. Flasks spiked with cadmium and 2,4-DCP solutions were also kept at pH 6.0 in an incubator using the method mentioned above.

Analytical and calculations

The initial and residual concentrations of Cd(II) concentration were measured using a flame atomic absorption spectrometry (FAAS) (PerkinElmer AA700, USA). The 2,4-DCP concentration in the aqueous solution was measured through a UV–visible spectrophotometer (Model UV-2550, Shimadzu, Japan) at 306 nm. An aqueous solution of 2,4-DCP with a basic pH had a stronger absorbance at 306 nm than that with a natural pH, and the basification could eliminate the interference in the analysis. Therefore, the sample was basified with a 2.0 mol/L NaOH solution (Chen et al. [2011a]).

The percentage removal and amount of removed Cd(II) or 2,4-DCP by the unit amount of PTNs (mg Cd(II)/g PTNs, or 2,4-DCP/g PTNs) were obtained by the following calculation:

$$\text{Removal rate}(\%) = \left(C - \frac{C}{C_0} \right) \times 100\% \qquad (1)$$

$$q = \frac{V}{M} \times (C_0 - C) \qquad (2)$$

where q (mg/g) is the amount of removed Cd(II) or 2,4-DCP by the unit amount of PTNs; C_0 and C (mg/L) are the concentrations of Cd(II) or 2,4-DCP in the solution before and after biosorption, respectively; V (L) is the volume of the aqueous solution; and M (g) is the weight of the PTNs. All experiments were done in triplicate and then analyzed with Origin 8.0 software or mapped with SigmaPlot 10.0.

Mechanism exploration

SEM (FEI QUANTA-200, FEI, Holland) photomicrographs were taken before and after the experiment to determine the morphological changes in the mycelium of PTNs. The energy distribution spectrum before and after the reaction was obtained using energy-dispersive X-ray analyzer (EDAX) (Vantage, NORAN, USA). Also, 20-kV acceleration voltage, 52 spot size, and 11-mm work distance were employed to observe the changes in the adsorption before and after the reaction.

In order to determine which functional groups were responsible for Cd(II) adsorption, an FT-IR analysis of the PTNs was carried out with an FT-IR spectrophotometer (WQF-410, China). The spectral range varied from 4,000 cm^{-1} to 400 cm^{-1}. The PTNs were dried at −40 °C in a freezer dryer (FD-1, Boyikang, Beijing, China). The dry PTNs (approximately 0.1 g) were mixed with KBr (0.1 g) and pressed into tablet form.

A GC–MS spectrometer (Model QP-2010 Ultra, Shimadzu, Japan) with a Rtx-50 capillary chromatographic column (30 m×0.25 mm×0.25 μm) was used to analyze the intermediates of 2,4-DCP in the degradation process. The injector type of the spectrometer is AOC-20i automatic sample injector. The solution with 20 mg/L Cd and 10 mg/L 2,4-DCP was selected to be treated with PTNs for 60 h. The solution was then extracted with dichloromethane three times, and the organic layer was collected for determination with GC–MS. The parameters used in the analysis were as follows: electron impact (EI) was used as an ionization technique with an electron energy of 70 eV and m/z ranging from 45 to 700. The ion source, injector port, and detector temperatures were 230, 250, and 280 °C, respectively. After starting under isothermal conditions at 45 °C for 2 min, the temperature was linearly raised 24 °C/min up to a maximum of 280 °C, which was maintained for 1 min.

Results

Effect of time

The effects of time on the Cd(II) biosorption and 2,4-DCP degradation by PTNs are shown in Fig. 1a and b, respectively. Based on Fig. 1a, the uptake of Cd(II) by PTNs, immobilized *P. chrysosporium* and immobilized nitrogen-doped TiO$_2$ nanoparticles all proceeded rapidly in the first few hours, accounting for about 98 % of total Cd(II) sorption. Few more Cd(II) was adsorbed with further increasing in contact time. The equilibrium time was 12 h for PTNs and immobilized *P. chrysosporium*, but 10 h for immobilized nitrogen-doped TiO$_2$ nanoparticles. It also showed that the ultimate removal rate of Cd(II) by PTNs (84.2 %) and immobilized *P. chrysosporium* (79.9 %) were higher than that by immobilized nitrogen-doped TiO$_2$ nanoparticles (53.9 %), which showed a high Cd(II) sorption ability of *P. chrysosporium*. As shown in Fig. 1b, the degradation efficiency of PTNs was superior to the other two materials. However, the equilibrium time of 2,4-DCP degradation by immobilized nitrogen-doped TiO$_2$ nanoparticles occurred at 12 h, whereas that was 60 h by PTNs and immobilized *P. chrysosporium*.
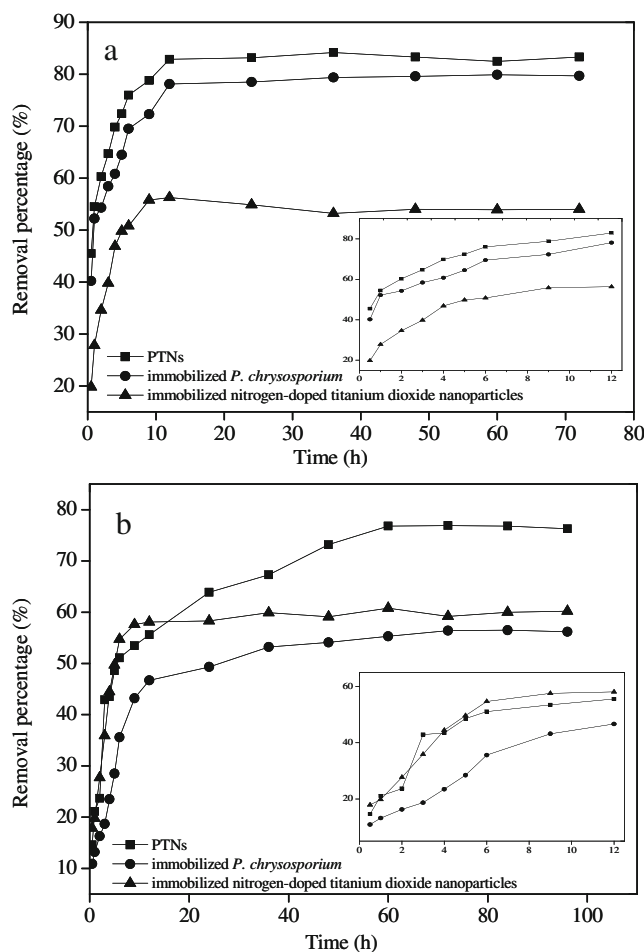
Fig. 1 Effect of initial pH on **a** Cd(II) removal and **b** 2,4-DCP degradation using PTNs, immobilized *P. chrysosporium*, and immobilized nitrogen-doped titanium dioxide nanoparticles, separately. The initial Cd(II) and 2,4-DCP concentrations were 20 and 10 mg/L, respectively. Initial pH was adjusted to 6.0. PTNs dosage was 9 g/L

Effect of pH

The sorption phenomenon at different pH varying from 3.0 to 8.0 is shown in Fig. 2. The removal rate of Cd(II) increased sharply from 36.9 % to 81.9 % as the pH increased from 3.0 to 4.0. However, minimal change was observed in the pH range of 4.0 to 7.0. The maximum Cd(II) sorption capacity reached 22.8 mg/g at pH 6.0. With a further increase of pH from 7.0 to 8.0, Cd(II) uptake ability decreased. As shown in Fig. 2, the degradation rate of 2,4-DCP increased slightly when the pH varied from 3.0 to 7.0 and decreased with an increasing alkalinity of the solution. The maximum degradation rate of 2,4-DCP was 78.3 % at pH 7.0.

Effect of initial Cd(II) concentration

The effect of initial Cd(II) concentration on Cd(II) sorption and 2,4-DCP degradation was examined using an initial 2,4-

Fig. 2 Effect of initial pH on Cd(II) removal 2,4-DCP degradation using PTNs at initial Cd(II) concentration of 20 mg/L and initial 2,4-DCP concentration of 10 mg/L. The initial pH in the medium was adjusted to 3.0, 4.0, 5.0, 6.0, 7.0 and 8.0, respectively. PTNs dosage was 9 g/L

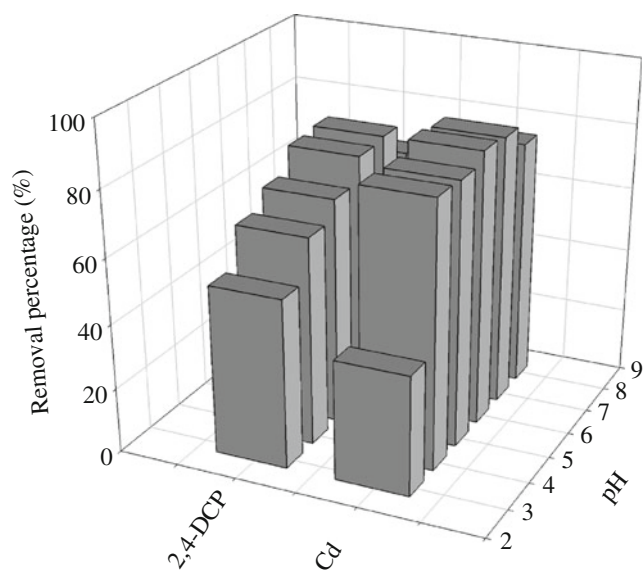Fig. 3 a Effect of initial Cd(II) concentration on Cd(II) removal and 2,4-DCP degradation using PTNs at initial pH 6.0 and initial 2,4-DCP concentration of 10 mg/L. The initial Cd(II) concentration in the medium was adjusted to 2, 5, 10, 20, 40, 60, 100, and 120 mg/L. b Effect of initial 2,4-DCP concentration on Cd(II) removal and 2,4-DCP degradation using PTNs at initial pH 6.0 and initial Cd(II) concentration of 20 mg/L. The initial 2,4-DCP concentration in the medium was adjusted to 2, 5, 10, 20, 40, 60, 80, and 100 mg/L

DCP concentration of 10 mg/L and Cd(II) concentration range of 5–120 mg/L (Fig. 3a). The adsorption capacity of Cd(II) increased with the adding of initial Cd(II) concentration, and it reached a plateau that represented the maximum uptake ability of PTNs (58.3 mg/g). Meanwhile, the removal rate of Cd(II) raised initially and subsequently declined with the variation of initial Cd(II) concentration. Additionally, there was no complete Cd(II) removal even under the lowest Cd(II) concentration. The maximum uptake rate of Cd(II) (84.5 %) was observed when the initial Cd(II) concentration was 20 mg/L. The results in Fig. 3a also showed that the initial Cd(II) concentration had an evident effect on 2,4-DCP degradation. Improvement of the initial Cd(II) concentration (below 40 mg/L) led to an enhancement of 2,4-DCP degradation capacity. The uptake rate of 2,4-DCP presented the same variation trend as the Cd(II) removal, but its maximum removal percentage (75.6 %) occurred at an initial Cd(II) concentration of 40 mg/L.

Effect of initial 2,4-DCP concentration

The effect of initial 2,4-DCP concentration on Cd(II) removal and 2,4-DCP degradation was illustrated over a 2,4-DCP concentration range of about 2–100 mg/L, using Cd(II) concentration of 20 mg/L to maintain a high Cd(II) uptake amount in Fig. 3b. It showed that the initial 2,4-DCP concentration had a significant influence on Cd(II) biosorption and 2,4-DCP degradation. The sorption capacity of Cd(II) decreased when the initial 2,4-DCP concentration was increased from 2 mg/L to 100 mg/L. However, the removal

rate of Cd(II) were 80.4 %, 81.6 %, 83.5 %, 84.8 %, 77.3 %, 68.5 %, 63.2 %, and 60.8 %, respectively. The 2,4-DCP degradation rate increased with an increase in the 2,4-DCP concentration of 2, 5, and 10 mg/L. However, a rapid decrease was observed when the initial 2,4-DCP concentration increased from 10 to 100 mg/L. The maximum removal rate of 2,4-DCP (72.6 %) occurred at an initial 2,4-DCP concentration of 10 mg/L. The change in 2,4-DCP degradation capacity presented the same trend as the variation of Cd(II) sorption capacity on initial 2,4-DCP concentration.

Mechanism exploration

The surface morphology of the PTNs before and after reacting with the composite wastewater was observed by SEM. As shown in Fig. 4, the PTNs were surrounded by *P. chrysosporium* hyphae with a network structure, which

Fig. 4 SEM images and EDAX spectra of PTNs: **a** in native form and **b** after reaction
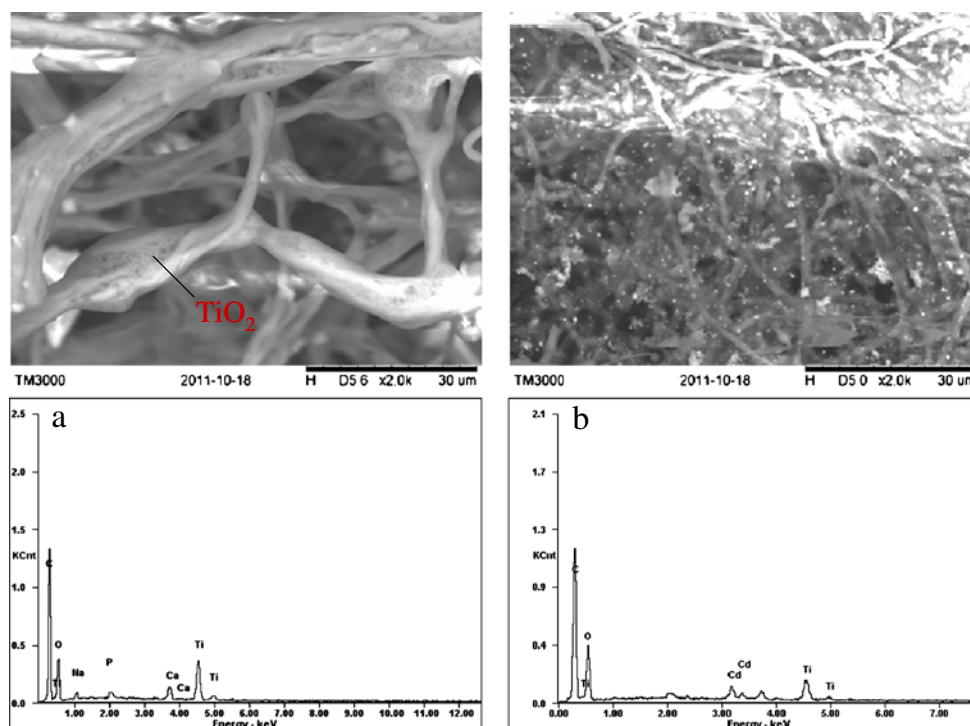
was propitious to the binding of Cd(II). After absorption, the PTNs became tight and a large amount of crystals adhered to them. The results in Fig. 4 also described the energy-dispersive X-ray analysis (EDAX) spectrum changes of the PTNs. The clear Cd peaks after reaction in the EDAX spectrum demonstrated that Cd(II) was adsorbed by the PTNs.

The functional groups responsible for heavy metal ion biosorption on PTNs is confirmed by FTIR spectra (Fig. 5). As shown in it, display of strong broad O–H stretch carboxylic bands or the stretching of –NH groups in the region $3{,}384$ cm^{-1} was observed. The peaks appearing in the region

$2{,}927$ and $2{,}858$ cm^{-1} could be assigned to the anti-symmetric and symmetric vibrations of CH$_2$ groups bound by the stretching of OH groups, whereas the peaks appearing in the region $1{,}739$ cm^{-1} might represent the carboxyl group. The peaks at $1{,}637$ cm^{-1}, $1{,}078$ cm^{-1}, and $1{,}034$ cm^{-1} represent the stretching vibration of carbonyl (amide I band), =C–O–C in aromatic and vinyl structures, C–N stretching of aliphatic amines, respectively (Chen et al. 2011a, b; Gupta and Rastogi 2008; Pang et al. 2011).

Although the residue concentration of 2,4-DCP strongly demonstrates the degradation ability of PTNs, the pathways and the catabolites of this new composite biomaterial are still unknown to us. GC–MS is an effective instrument that can detect various organics in specific organic solvent, thus degradation intermediates may be confirmed and the pathways may be conjectured (Fig. 6). As shown in it, several intermediates emerged, e.g., *o*-chlorotoluene, 4-hexene-1-ol after reacted with PTNs for 60 h. Based on these intermediates, combining the degradation mechanisms of fungus and photochemistry illustrated in other articles, brief degradation pathways were concluded (Fig. 6).

Fig. 5 FTIR spectra of PTNs: **a** in native form and **b** after reaction

Discussion

Equilibrium time is one of the most vital parameters that impact a new biomaterial to be used in the practical application. Contact time experiments not only gave out the

Fig. 6 GC–MS spectra of solution containing 20 mg/L Cd (II) and 10 mg/L 2,4-DCP after reaction with PTNs and the degradation pathways

proper reaction time but also proved that the PTNs obtained in the current research were effective for the removal of Cd (II) from composite-polluted wastewater. Fungus has a mass of functional groups and hyphae with a network structure to adsorb heavy metals, which is a mixed effect of physics and chemistry force. However, the heavy metal uptake ability of nitrogen-doped TiO_2 is mainly a physical effect with the aid of its large specific surface area. Also, immobilization of TiO_2 reduced its adsorption capacity to some extent. Thus, the uptake rate of PTNs and immobilized *P. chrysosporium* was higher than immobilized nitrogen-doped TiO_2 nanoparticles. Difference in reaction rate of microorganism and chemical material led to their diverse Cd(II) uptake equilibrium time. The decomposing of 2,4-DCP was related to (1) the photocatalysis of nitrogen-doped TiO_2 nanoparticles and (2) the biodegradation of *P. chrysosporium* with the help of enzymes (Yin et al. 2010b). The decomposing rate of photocatalysis was faster than the biodegradation by fungus (Antoniadou et al. 2011; Quan et al. 2007). Thus, the equilibrium time of PTNs was between immobilized *P. chrysosporium* and nitrogen-doped TiO_2 nanoparticles.

The effects of the initial pH on the cadmium removal and 2,4-DCP degradation were evaluated within the pH range of 3.0–8.0. Most of the Cd(II) precipitates in the form of Cd $(OH)_2$ if the pH surpasses 8.0. Too many hydronium ions in the solution can compete with the Cd(II) to combine with the functional groups on the surface of PTNs. Hence, a pH lower than 3.0 or higher than 8.0 was not considered in this study.

Functional groups on the surface of PTNs, such as hydroxyl (R–OH), carboxyl (R–COOH), and sulfate groups $(R–OSO_3^-)$, play important roles on the sorption of Cd(II) (Chen et al. 2006; Gupta and Rastogi 2008). Most of the functional groups were highly protonated at strongly acid conditions and firmly repulsed the Cd(II). This phenomenon may explain the low sorption of Cd(II) seen at pH 3.0 in the current study. With the decrease of acidity, negatively charged groups on PTNs, such as carboxyl and sulfate groups, were more abundant. Thus, the increase in

electrostatic attractions between positively charged Cd(II) and negatively charged binding sites led to a high Cd(II) removal rate in the range of 4.0 to 7.0. On the other side, nitrogen-doped TiO_2 nanoparticles also played a part in Cd (II) removal, and the sorption of Cd(II) by nanoparticles was not pH dependent and uptake ability remained high except in extreme condition (pH 3.0). Nitrogen-doped TiO_2 nanoparticles played a major role in pH 4.0–5.0 and functional groups on the surface of PTNs in pH 6.0–7.0. Thus, these two effects functioned together, leading to a high Cd(II) removal rate in the range of 4.0 to 7.0. These results were in agreement with previous studies. For example, Kim et al. (2003) investigated the removal of heavy metals using anatase-type TiO_2 and found that the sorption capacity of TiO_2 was almost the same at pH 4.0 to 7.0, similar to results reported by Bakircioglu et al. (2010).

Several studies suggested that the surface of nitrogen-doped TiO_2 nanoparticles carries a net positive charge at low pH conditions, whereas chlorophenols and intermediates were negatively charged in nature. Therefore, low pH could facilitate the adsorption of organic compounds and promote photocatalytic degradation (Quan et al. 2007; Sun et al. 2008). However, other studies supposed that there were more hydroxide ions in the solution with high pH, and these would react with the valence band holes to form hydroxyl radicals, subsequently to enhance the degradation rate of TiO_2 nanoparticles (Doong et al. 2001; Liang et al. 2008). There were two possible reasons for the increasing degradation of 2,4-DCP with the increase of pH in the current study: (1) nitrogen-doped TiO_2 nanoparticles were loaded in *P. chrysosporium*; thus, the sorption of 2,4-DCP could be ignored. (2) The degradation effect of *P. chrysosporium* was related to the stability and activity of enzymes (Yin et al. 2010b). The enzymes secreted by *P. chrysosporium* were mainly stabilized by weak interactions, such as hydrogen bonds, van der Waals' forces, etc., which were largely influenced by the pH of the medium. An increase or decrease in the pH beyond a certain range adversely affected

the stability and activity of the enzymes, thereby decreasing the degradation rate of 2,4-DCP (Chen et al. 2011a).

The sorption capacity of Cd(II) improved with an increase in the initial Cd(II) concentration. A high initial Cd(II) concentration enhanced the mass transfer driving force between PTNs and the fluid phase (Chen et al. 2008). Moreover, an elevated initial Cd(II) concentration increased the collision chances between PTNs and Cd(II), which also enhanced the adsorption processes (Rathinam et al. 2010; Chen et al. 2011a). The lower removal percentage of Cd(II) at high initial Cd(II) concentration could be due to the competition of more metal ions for a fixed amount of available binding sites or a lower ratio of metal ions to adsorption sites (Khoo and Ting 2001). The degradation of 2,4-DCP improved with the increase of initial Cd(II) concentration below 40 mg/L, which may be the effect of CdS synthesized by high initial Cd(II) concentration and sulfur released from *P. chrysosporium*. CdS is an important functional photocatalyst under visible light and can decompose many kinds of compounds alone or in combination with other photocatalysts. Combined photocatalysts show a better effect than pure CdS (Jaussaud et al. 2000). Moreover, Cd(II) may be loaded on titania to enhance the photocatalytic ability of PTNs under visible light (Antoniadou et al. 2011). However, when the Cd(II) concentration was over 40 mg/L, the degradation effect of *P. chrysosporium* was inhibited by toxic heavy metals, resulting in reduced 2,4-DCP degradation (Song et al. 2009).

An increase with the initial 2,4-DCP concentration enhanced Cd(II) removal up to an optimum level of 10 mg/L. This finding was due to the appearance of low molecular carbon compounds as intermediates during the degradation process (Yin et al. 2010a, b; Jaussaud et al. 2000). These low molecular carbon compounds may be used as a carbon and energy source by *P. chrysosporium* to improve the activity of *P. chrysosporium* and the secretion of enzyme, thus promoting Cd(II) sorption and 2,4-DCP degradation. However, an excessive amount of 2,4-DCP would poison the PTNs and lessen their activity, leading to a decrease of Cd(II) biosorption at an initial 2,4-DCP concentration of over 10 mg/L (Song et al. 2009; Chen et al. 2011a). The variation of 2,4-DCP degradation capacity with the increase of initial 2,4-DCP concentration may also be the mass transfer limitation and collisions explained above.

The early strong indications of ion exchange being at the root of biosorption metal uptake led us to examine the active chemical groups involved in the metal binding. FT-IR is an important tool to identify the functional groups in materials, which were capable of adsorbing metal ions. The broad absorption peak around 3,384 cm^{-1} indicated the existence of bound hydroxyl or –NH groups, and the shift from 3,384 cm^{-1} to 3,388 cm^{-1} demonstrated that the hydroxyl groups changed from multimer to monopolymer or even to a

dissociative state, which meant that the degree of the hydroxyl polymerization in the PTNs decreased with the addition of Cd(II) (Xiao et al. 2010). Furthermore, the characteristic peak of the stretching vibration of carbonyl (amide I band) at 1,637 cm^{-1} shifted by approximately 13 cm^{-1} after the reaction and the intensity was strengthened. This is due to the formation of nitrogen oxide in Cd(II) reduction by PTNs. Another change in the spectrum was that of the carboxyl group: its adsorption peak shifted from around 1,739 cm^{-1} to 1,738 cm^{-1} after reaction, which indicated that the C=O groups present in the PTNs were also responsible for the biosorption of cadmium (Pang et al. 2011; Gupta and Rastogi 2008).

With the aid of GC–MS, the possible degradation pathways of 2,4-DCP by PTNs under the existence of Cd(II) were obtained. When nitrogen-doped TiO_2 nanoparticles were illuminated by visible light, hydroxyl radicals were generated in the solution. Thus, oxidation reactions started at the aromatic hydroxylation (Yin et al. 2010a, b). The attack of hydroxyl radicals occurs most favorably at the para and ortho positions due to the electron-donating behavior of the phenolic OH group and the electrophilicity of hydroxyl radicals (Lu et al. 2006). As shown in Fig. 6, chlorine atoms were displaced from the benzene rings, generating *o*-chlorotoluene first and then 1,3-dimethyl benzene. Benzene rings were broken down into low-toxicity organics with a linear chain, producing 4-hexene-1-ol and 2-sulfydryl-1-methyl pentane. Then these low-molecule organics would be further decomposed by *P. chrysosporium*. Eventually, all these organics would be completely degraded into CO_2 and H_2O.

In conclusion, immobilized *P. chrysosporium* loaded with nitrogen-doped TiO_2 nanoparticles presented an excellent remediation agent for simultaneous Cd(II) biosorption and 2,4-DCP degradation by enhancing resistance to the toxics and shortening the degradation time of *P. chrysosporium*. High removal capacity was obtained within a wide pH range from 4.0 to 7.0. The maximum removal efficiencies reached 84.2 % for Cd and 78.9 % for 2,4-DCP under the initial concentrations of 20 mg/L Cd(II) and 10 mg/L 2,4-DCP. After the reaction, Cd(II) was mainly bound to carboxyl, amino, and hydroxyl groups on the surface of PTNs. 2,4-DCP was degraded into low-molecular carbon compounds under the function of TiO_2 nanoparticles and *P. chrysosporium*. These results indicated the potential application of PTNs to remediate composite-polluted wastewater with heavy metals and organics.

References

Andreozzi R, Somma DI, Marotta R, Pinto G, Pollio A, Spasiano D (2011) Oxidation of 2,4-dichlorophenol and 3,4-dichlorophenol by means of Fe(III)-homogeneous photocatalysis and algal toxicity assessment of the treated solutions. Water Res 45:2038–2048

Antoniadou M, Daskalaki VM, Balis N, Kondarides DI, Kordulis C, Lianos P (2011) Photocatalysis and photoelectrocatalysis using (CdS-ZnS)/TiO$_2$ combined photocatalysts. Appl Catal, B 107:188–196

Asahi R, Morikawa T, Ohwaki T, Aoki K, Taga Y (2001) Visible-light photocatalysis in nitrogen-doped titanium oxides. Science 293:269–271

Bakircioglu Y, Bakircioglu D, Akman S (2010) Biosorption of lead by filamentous fungal biomass-loaded TiO$_2$ nanoparticles. J Hazard Mater 178:1015–1020

Brezová V, Vrecková Z, Billik P, Čaplovičová M, Plesch G (2009) Photoactivity of mechanochemically prepared nanoparticulate titanium dioxide investigated by EPR spectroscopy. J Photochem Photobiol A 206:177–187

Chen GQ, Zeng GM, Tu X, Niu CG, Huang GH, Jiang W (2006) Application of a by-product of *Lentinus edodes* to the bioremediation of chromate contaminated water. J Hazard Mater 135:249–255

Chen GQ, Zeng GM, Tang L, Du CY, Jiang XY, Huang GH, Liu HL, Shen GL (2008) Cadmium removal from simulated wastewater to biomass byproduct of *Lentinus edodes*. Bioresour Technol 99:7034–7040

Chen AW, Zeng GM, Chen GQ, Fan JQ, Zou ZJ, Li H, Hu XJ, Long F (2011a) Simultaneous cadmium removal and 2,4-dichlorophenol degradation from aqueous solutions by *Phanerochaete chrysosporium*. Appl Microbiol Biotechnol 91:811–821

Chen GQ, Zou ZJ, Zeng GM, Yan M, Fan JQ, Chen AW, Zhang WJ, Wang L (2011b) Coarsening of extracellularly biosynthesized cadmium crystal particles induced by thioacetamide in solution. Chemosphere 83:1201–1207

Doong RA, Chen CH, Maithreepala RA, Chang SM (2001) The influence of pH and cadmium sulfide on the photocatalytic degradation of 2-chlorophenol in titanium dioxide suspensions. Water Res 35:2873–2880

Gimeno O, Rivas FJ, Beltran FJ, Carbajo M (2007) Photocatalysis of fluorene adsorbed onto TiO$_2$. Chemosphere 69:595–604

Gupta VK, Rastogi A (2008) Sorption and desorption studies of chromium(VI) from nonviable cyanobacterium *Nostoc muscorum* biomass. J Hazard Mater 154:347–354

Huang DL, Zeng GM, Feng CL, Hu S, Jiang XY, Tang L, Su FF, Zhang Y, Zeng W, Liu HL (2008) Degradation of lead-contaminated lignocellulosic waste by *Phanerochaete chrysosporium* and the reduction of lead toxicity. Environ Sci Technol 42:4946–4951

Jaussaud C, Païssé O, Faure R (2000) Photocatalysed degradation of uracil in aqueous titanium dioxide suspensions: mechanisms, pH and cadmium chloride effects. J Photochem Photobiol A 130:157–162

Jo WK, Kim WK (2009) Application of visible-light photocatalysis with nitrogen-doped or unmodified titanium dioxide for control of indoor-level volatile organic compounds. J Hazard Mater 164:360–366

Khoo KM, Ting YP (2001) Biosorption of gold by immobilized fungal biomass. Biochem Eng J 8:51–59

Kim MS, Hong KM, Chung JG (2003) Removal of Cu(II) from aqueous solutions by adsorption process with anatase-type titanium dioxide. Water Res 37:3524–3529

Liang HC, Li XZ, Yang YH, Sze KH (2008) Effects of dissolved oxygen, pH, and anions on the 2,3-dichlorophenol degradation by photocatalytic reaction with anodic TiO$_2$ nanotube films. Chemosphere 73:805–812

Lu QF, Yu J, Gao JZ (2006) Degradation of 2,4-dichlorophenol by using glow discharge electrolysis. J Hazard Mater 136:526–531

Pang Y, Zeng GM, Tang L, Zhang Y, Liu YY, Lei XX, Li Z, Zhang JC, Xie GX (2011) PEI-grafted magnetic porous powder for highly effective adsorption of heavy metal ions. Desalination 281:278–284

Prasad K, Pinjari DV, Pandit AB, Mhaske ST (2010) Synthesis of titanium dioxide by ultrasound assisted sol–gel technique: effect of amplitude (power density) variation. Ultrason Sonochem 17:697–703

Quan X, Ruan XL, Zhao HM, Chen S, Zhao YZ (2007) Photoelectrocatalytic degradation of pentachlorophenol in aqueous solution using a TiO$_2$ nanotube film electrode. Environ Pollut 147:409–414

Rathinam A, Maharshi B, Janardhanan SK, Jonnalagadda RR, Nair BU (2010) Biosorption of cadmium metal ion from simulated wastewaters using *Hypnea valentiae* biomass: a kinetic and thermodynamic study. Bioresour Technol 101:1466–1470

Sayari A, Hamoudi S, Yang Y (2005) Applications of pore-expanded mesoporous silica. 1. Removal of heavy metal cations and organic pollutants from wastewater. Chem Mater 17:212–216

Song HX, Liu YG, Xu WH, Zeng GM, Aibibu N, Xu L, Chen BB (2009) Simultaneous Cr(VI) reduction and phenol degradation in pure cultures of *Pseudomonas aeruginosa* CCTCC AB91095. Bioresour Technol 100:5079–5084

Sun JH, Qiao LP, Sun SP, Wang GL (2008) Photocatalytic degradation of Orange G on nitrogen-doped TiO$_2$ catalysts under visible light and sunlight irradiation. J Hazard Mater 155:312–319

Wodka D, Bielanska E, Socha RP, Elzbieciak-Wodka M, Gurgul J, Nowak P, Warszynski P, Kumakiri I (2010) Photocatalytic activity of titanium dioxide modified by silver nanoparticles. Appl Mater Interfaces 2:1945–1953

Xiao X, Luo SL, Zeng GM, Wei WZ, Wan Y, Chen L, Guo HJ, Cao Z, Yang LX, Chen JL, Xi Q (2010) Biosorption of cadmium by endophytic fungus (EF) *Microsphaeropsis* sp. LSE10 isolated from cadmium hyperaccumulator *Solanum nigrum* L. Bioresour Technol 101:1668–1674

Yin LF, Niu JF, Shen ZY, Chen J (2010a) Mechanism of reductive decomposition of pentachlorophenol by Ti-doped β-Bi$_2$O$_3$ under visible light irradiation. Environ Sci Technol 44:5581–5586

Yin LF, Shen ZY, Niu JF, Chen J, Duan YP (2010b) Degradation of pentachlorophenol and 2,4-dichlorophenol by sequential visible-light driven photocatalysis and laccase catalysis. Environ Sci Technol 44:9117–9122

Zhang ZC, Brown S, Goodall JBM (2009) Direct continuous hydrothermal synthesis of high surface area nanosized titania. J Alloy Comp 476:451–456

Zouari H, Labat M, Sayadi S (2002) Degradation of 4-chlorophenol by the white rot fungus *Phanerochaete chrysosporium* in free and immobilized cultures. Bioresour Technol 84:145–150

Zumriye A, Gönen F (2006) Binary biosorption of phenol and chromium (VI) onto immobilized activated sludge in a packed bed: prediction of kinetic parameters and breakthrough curves. Sep Purif Technol 49:205–216